^{1}H NMR Studies on Strongly Antiferromagnetically Coupled Dicopper(II) Systems

Anbanandam Asokan and Periakaruppan T. Manoharan*,†

Department of Chemistry and Regional Sophisticated Instrumentation Centre, Indian Institute of Technology Madras, Chennai-600036, India

Received March 25, 1998

The ^{1}H NMR spectra of three well-characterized μ-phenoxo and μ-hydroxo spin coupled dicopper(II) complexes **1**, **2**, and **3** which are strongly antiferromagnetically coupled in the solid state have been studied in solution. The complexes studied were $[(Cu_2(DAP)_2IPA)(OH)(H_2O)](ClO_4)_2 \cdot H_2O$ (**1**) (DAP = 1,3-diaminopropane; IPA = 2-hydroxy-5-methylisophthalaldehyde), $[(Cu_2(DMDAP)_2IPA)(OH)(H_2O)](ClO_4)_2$ (**2**) (DMDAP = *N*,*N*-dimethyl-1,3-diaminopropane), and $[(Cu_2(AEP)_2IPA)(OH)(H_2O)](ClO_4)_2$ (**3**) (AEP = 2-(2-aminoethyl)pyridine). All three complexes exhibit relatively sharp hyperfine shifted NMR signals. Signal assignments were based on intensity and T_1 values. An analysis of the relaxation data shows that, for these binuclear copper(II) systems, the reorientational correlation time (τ_c) is dominated probably by a combination of electronic relaxation τ_s and rotational correlation time (τ_r) due to an exchange-modulated dipolar mechanism. The temperature dependence of the isotropic shifts has been interpreted in terms of the contact hyperfine interaction constant (A) and exchange coupling constant ($-2J$). The fitting of these shifts represents a good method for the evaluation of $-2J$ in solution, which is compared to the solid state $-2J$ value obtained by the SQUID method. The results indicate that the structures and magnetic properties of all three complexes (**1**−**3**) support a general correlation with the antiferromagnetic coupling constants as evidenced by both solid and solution studies. Our results show that ^{1}H NMR spectroscopy is an excellent tool to probe the solution structures of magnetically coupled binuclear Cu(II) centers in model complexes as well as biological systems. One of these complexes was crystallized from aqueous solution. The crystal and molecular structure of $[(Cu_2(DMDAP)_2IPA)(OH)(H_2O)](ClO_4)_2$ (**2**) has been determined. This crystallizes in the monoclinic system, space group *Cc* with formula weight = 692.48, a = 12.472(2) Å, b = 19.554(2) Å, c = 12.185(12) Å, β = 107.48 (9)°, Z = 4. The two Cu atoms in this copper(II) complex are bridged by the oxygen atoms of the phenolate and hydroxy groups. The axial position at one Cu atom is occupied by a water molecule, while another Cu has weak interaction with a perchlorate group. The coordination geometries around the two Cu atoms are distorted square pyramidal and square planar.

Introduction

Interest in binuclear centers has focused primarily on magnetic exchange (spin−spin) interaction between two paramagnetic (s = $^1/_2$) cupric ions.[1−3] Such interactions in biomolecules have received increased focus since the time binuclear copper centers were proposed to be part of the active site of several multicopper-containing proteins.[4,5] The "type 3" copper in Laccase consists of a pair of antiferromagnetically coupled Cu(II) ions[4] which are capable of acting as two electron oxidants. Mason[5] has reviewed the evidence for binuclear copper centers in a variety of proteins.

In the case of binuclear metal complexes the coupling between the electrons of the two metal ions leads to low-lying states of different spin multiplicities, which can be populated at thermal energies ($\leq$500 cm^{-1}). The resulting magnetic behavior will be antiferromagnetic or ferromagnetic depending on whether the low-spin or high-spin state is the ground state, respectively. Systematic observation of such interactions even in the early 1960s and 1970s[6−10] has been interpreted in terms of a superexchange mechanism via ligand entities that bridge the two metal centers.[11,12] Both single-atom and multiatom bridges are known to propagate exchange with the magnitude of exchange interaction being dependent upon the bridge identity, its length, the angle subtended at the bridge, the metal bridge ligand bond lengths, the metal ion stereochemistry, etc. Most of the theoretical work for the understanding of the exchange mechanism is based on the works of Kramers,[13] Anderson,[14] Goodenough,[15] and Kanamori.[16] Extensive theoretical work has come from the groups of Hay et al.,[17] Bencini

* Author to whom correspondence should be addressed.
† E-mail: ptm@magnet.iitm.ernet.in. Fax: 91-44-2350509.

(1) Hatfield, W. E. *ACS Symp. Ser.* **1975**, No. 5, 108.
(2) Hodgson, D. J. *Prog. Inorg. Chem.* **1975**, *19*, 173.
(3) Pierpont, C. G.; Francesconi, L. C.; Hendrickson, D. N. *Inorg. Chem.* **1977**, *16*, 2367.
(4) Malkin, R.; Malstrom, B. G. *Adv. Enzymol.* **1970**, *33*, 177.
(5) Mason, H. S. In *Iron and Copper proteins*; Yasunoba, K. T., Mower, H. F., Hayaishi, O., Eds.; Plenum: New York, 1976; p 464.
(6) Kato, M.; Jonassen, H. B.; Fauning, J. C. *Chem. Rev.* **1964**, *64*, 99.
(7) Martin, R. L. In *New pathways in Inorganic Chemistry*; Ebsworth, E. A. V., Meddock, A. G., Sharpe, A. G., Eds.; Cambridge University Press: London, 1968; Chapter 9.
(8) Ball, P. W. *Coord. Chem. Rev.* **1969**, *4*, 361.
(9) Ginsberg, A. P. *Inorg. Chim. Acta, Rev.* **1971**, *5*, 45.
(10) Gray, H. B. *Adv. Chem. Ser.* **1971**, No. 100, 365.
(11) Willett, R. D. In *Magnetostructural Correlations in exchange coupled systems*; Willett, R. D., Gatteschi, D., Kahn, O., Eds.; Reidel: Dordrecht, 1985; p 389.
(12) Hendrickson, D. N. In *Magnetostructural Correlations in exchange coupled Systems*; Willett, R. D., Gatteschi, D., Kahn, O., Eds.; Reidel: Dordrecht, 1985; p 523.
(13) Kramers, H. A. *Physica* **1934**, *1*, 182.
(14) Anderson, P. W. *Phys. Rev.* **1950**, *79*, 350.
(15) Goodenough, J. B. *Phys. Rev.* **1955**, *100*, 564.
(16) Kanamori, J. *Phys. Chem. Solids* **1959**, *10*, 87.
(17) Hay, P. J.; Thibeault, J. C.; Hoffmann, R. *J. Am. Chem. Soc.* **1975**, *97*, 4884.

10.1021/ic9803356 CCC: $18.00
Published on Web 11/18/1999

and Gatteschi,[18] de Loth,[19] and Comarmond.[20] Recently diagrammatic valence bond theory[21,22] and DFT[23] have been used for the understanding of the exchange mechanism.

Although different experimental techniques, such as magnetic susceptibility, EPR, etc., have been used to derive the details of exchange interactions in solids, detailed studies on exchange interactions in solution have been rather few.[24−33] Exchange interactions in solution are not easy to measure. This difficulty arises due to the loss of solid state packing. However, even if the integrity of the metal cluster is not disturbed in solution, a general application of a methodology becomes difficult due to other reasons such as sign and magnitude of exchange interaction. This makes most methods inapplicable.

Though ^{1}H NMR spectroscopy is not generally viewed as a viable solution characterization technique for paramagnetic Cu(II) complexes because of the inherently slow electronic relaxation of copper(II),[32] the situation is different in magnetically coupled multinuclear systems. A consequence of magnetic coupling can be a change in the electronic relaxation times of the involved metal ions. Magnetic coupling gives rise to new energy levels which can provide new relaxation pathways in binuclear and polymetallic systems.[33]

NMR spectroscopy has been widely used as a versatile technique to elucidate the structure and magnetic properties of antiferromagnetically coupled binuclear iron complexes[33,34] as well as copper(II) coupled with fast relaxing metal ions such as iron[35] and cobalt[36] and also with free radical ligands.[37] However, the determination of the structural and magnetic properties of binuclear copper(II) complexes using NMR spectroscopy is less common in the literature.[28,29,30]

In addition, the NMR spectra of binuclear complexes in solution provide information on the role of the ligands in the superexchange pathway as well as the electronic state of the coupled metal centers.[34,38] It can also provide information about the structure of the complexes in solution and the distribution of the unpaired electrons. It can be seen therefore that NMR studies on binuclear complexes can be a rich source of information.

Nuclear relaxation has been used to characterize the structure and dynamics of the molecules. Particularly in the case of paramagnetic molecules, determination of coordination number and correlation times have been inferred from the investigation of paramagnetic relaxation.[39] However, the relaxation mechanisms are modified when there is exchange interaction between the electron spins of the metal ions present in the moiety. Understanding the effect of magnetic coupling on nuclear relaxation parameters is relevant to several biological systems where such couplings are known (iron−sulfur proteins, cytochrome oxidase) to occur. Efforts have been made by Bertini and co-workers[30,40,41] to study the relaxational (T_1) properties of systems with weak exchange coupling. The present report includes the detailed and quantitative analysis of relaxational properties of the strongly antiferromagnetically coupled binuclear copper(II) complexes.

The purpose of our work is to analyze the NMR spectra of isotropically shifted signals of three (schematic representations of the complexes are shown in Figure 1) strongly antiferromagnetically coupled binuclear Cu(II) complexes. On the basis of these spectra, the structures in solution are discussed and are simultaneously compared with the X-ray crystallographic structures determined, and in this paper we report the X-ray crystallographic molecular structure for one such complex. We have made an attempt to compare the exchange coupling constant ($-2J$) measured in both the solid and solution states. In the solution state, exchange coupling constants are calculated by using chemical shift as a function of temperature. Here, we have also addressed a possible mechanism for relaxation of two of the three strongly antiferromagnetically coupled dicopper(II) systems by combining the signal assignment with X-ray crystallographic results and T_1 values. Our data indicate that ^{1}H NMR spectroscopy is an excellent tool to probe the binuclear Cu(II) systems in solution in line with some of the more recent works.[29,30,32]

Experimental Section

CAUTION! Perchlorate complexes of metal ions are potentially explosive. Only a small amount of material should be prepared, and it should be handled with caution.

Synthetic Methods. All chemicals were purchased commercially and used as received unless otherwise stated.

[(Cu_2(DAP)$_2$IPA)(OH)(H_2O)](ClO_4)$_2$·H_2O (1). The title complex was prepared by the method of Mandal and Nag.[42] A mixture of 2-hydroxy-5-methylisophthalaldehyde (IPAH) (1.64 g, 10 mmol), NaOH (0.4 g, 10 mmol), and water (5 cm^3) was ground to a paste in a mortar. This was added with stirring to boiling water (1 dm^3), and a clear yellow solution was obtained. A second solution of $Cu(ClO_4)_2$·

(18) Bencini, A.; Gatteschi, D. *Inorg. Chim. Acta* **1978**, *31*, 11.
(19) de Loth, P.; Caussoux, P.; Dandey, J. P.; Malrieu, J. P. *J. Am. Chem. Soc*. **1981**, *103*, 4007.
(20) Comarmond, J.; Plumere, P.; Lehn, J. M.; Agnus, Y.; Lousis, R.; Weiss, E. Kahn, O.; Morgenstern, B. I. *J. Am. Chem. Soc*. **1982**, *104*, 6330.
(21) Ramasesha, S.; Rao, C. N. R. *Phys. Rev*. **1991**, *B44*, 7046.
(22) (a) Mandal P. K.; Sinha, B.; Manoharan, P. T.; Ramasesha, S. *Chem. Phys. Lett*. **1992**, *191*, 448. (b) Mandal, P. K.; Manoharan, P. T. *Chem. Phys. Lett*. **1993**, *210*, 463.
(23) (a) Ruiz, E.; Alemany, P.; Alvarez, S.; Cano, J. *J. Am. Chem. Soc*. **1997**, *119*, 1297. (b) Ruiz, E.; Alemany, P.; Alvarez, S.; Cano, J. *Inorg. Chem*. **1997**, *36*, 3683.
(24) Byers, W.; Williams, R. J. P. *J. Chem. Soc*. **1973**, 555.
(25) Dei, A.; Gatteschi, D.; Piergentili, E. *Inorg. Chem*. **1979**, *18*, 89.
(26) Zelonka, R. A.; Baird, M. C. *Inorg. Chem*. **1972**, *11*, 134.
(27) Maekawa, M.; Kitagawa, S.; Munakata, M.; Masuda, H. *Inorg. Chem*. **1989**, *28*, 1904.
(28) (a) Mandal, P. K.; Manoharan P. T. *Inorg. Chem*. **1995**, *34*, 270. (b) Asokan, A.; Mandal, P. K.; Varghese, B.; Manoharan, P. T. *Proc. Indian Acad. Sci. (Chem. Sci.)* **1995**, *107*, 281.
(29) (a) Holz, R. C.; Brink, J. M. *Inorg. Chem*. **1994**, *33*, 4609. (b) Holz, R. C.; Brink, J. M.; Gobena, F. T.; O'Conner, C. J. *Inorg. Chem*. **1994**, *33*, 6086. (c) Brink, J. M.; Rose, R. A.; Holz, R. C. *Inorg. Chem*. **1996**, *35*, 2878.
(30) Murthy, N. N.; Karlin, K. D.; Bertini, I.; Luchinat, C. *J. Am. Chem. Soc*. **1997**, *119*, 2156.
(31) Holz, R. C.; Brink, J. M.; Rose, R. A. *J. Magn. Reson*. **1995**, *119*, 125.
(32) Satcher, J. H.; Balch, A. L. *Inorg. Chem*. **1995**, *34*, 3371.
(33) (a) Bertini, I.; Luchinat, C. *NMR of paramagnetic Molecules in Biological Systems*; Benjamin and Cummings: Menlo Park, CA, 1986. (b) Bertini, I.; Luchinat, C. *Coord. Chem. Rev*. **1996**, *150*, Chapter 5. (c) Bertini, I.; Turano, P.; Vila, A. J. *Chem. Rev*. **1993**, *93*, 2833.
(34) (a) La Mar, G. N.; Eaton, G. R.; Holm, R. H.; Walker, F. A. *J. Am. Chem. Soc*. **1972**, *95*, 63. (b) La Mar, G. N.; de Ropp, J. S. *NMR methodology for paramagnetic proteins*; Plenum Press: New York, 1993; Vol. 12, p 1.
(35) Karlin, K. D.; Nanthakumar, A.; Fox, S.; Murthy, N. N.; Ravi, N.; Huynh, B. H.; Orasz, R. D.; Day, E. P. *J. Am. Chem. Soc*. **1994**, *116*, 4753.
(36) (a) Bertini, I.; Lainini, G.; Luchinat, C.; Messori, L.; Scozzafava, A. *J. Am. Chem. Soc*. **1985**, *107*, 4391. (b) Banci, L.; Bertini, I.; Luchinat, C.; Piccioli, M.; Scozzafava, A.; Turano, P. *Inorg. Chem*. **1989**, *28*, 4650.
(37) Balch, A. L.; Mazzanti, M.; Noll, B. C.; Olmstead, M. M. *J. Am. Chem. Soc*. **1993**, *115*, 12206.
(38) Wicholas, M. *J. Am. Chem. Soc*. **1970**, *92*, 4141.
(39) Yamamoto, Y.; Nanai, N.; Chujo, R. *Bull. Chem. Soc. Jpn*. **1991**, *64*, 3199.
(40) Owens, C.; Drago, R. S.; Bertini, I.; Luchinat, C.; Banci, L. *J. Am. Chem. Soc*. **1986**, *108*, 3298.
(41) Banci, L.; Bertini, I.; Luchinat, C.; Scozzafava, A. *J. Am. Chem. Soc*. **1987**, *109*, 2328.
(42) Mandal, S. K.; Nag, K. *J. Chem. Soc., Dalton Trans*. **1984**, 2141.

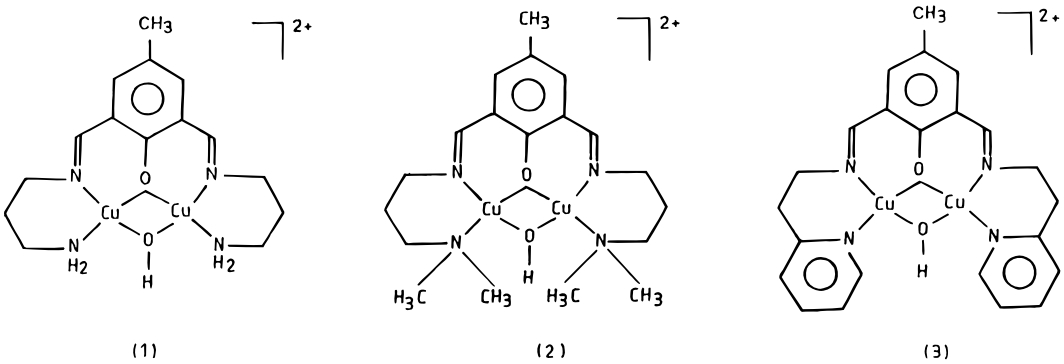

Figure 1. Schematic representations of $[(Cu_2(DAP)_2IPA)(OH)(H_2O)](ClO_4)_2 \cdot H_2O$ (**1**), $[(Cu_2(DMDAP)_2IPA)(OH)(H_2O)](ClO_4)_2$ (**2**), and $[(Cu_2(AEP)_2IPA)(OH)(H_2O)](ClO_4)_2$ (**3**).

$6H_2O$ (9.3 g, 25 mmol) and 1,3-diaminopropane (DAP) (2.2 g, 30 mmol) in water (50 cm^3) was added to the first solution and boiled. The resulting deep blue solution was concentrated on a hot plate. When the volume of the solution had been reduced to ca. 25 cm^3, it was filtered hot. The filtrate was allowed to cool at ambient temperature and the blue crystalline product collected by filtration. The product was further recrystallized from boiling water and dried over $CaCl_2$.

$[(Cu_2(DMDAP)_2IPA)(OH)(H_2O)](ClO_4)_2$ (2). This complex was prepared in essentially the same way as **1** using (2.5545 g, 25 mmol) *N*,*N*-dimethyl-1,3-diaminopropane (DMDAP).

$[(Cu_2(AEP)_2IPA)(OH)(H_2O)](ClO_4)_2$ (3). This complex was prepared by the literature method.[43]

Physical Measurements. ^{1}H NMR. All ^{1}H NMR spectra were recorded on a JEOL JNM-GSX 400 MHz FT-NMR machine using a 7.2 μs 90° pulse width, a 98 kHz spectral width, and a 3 s delay between 90° pulses. Chemical shifts (ppm) are reported with respect to tetramethylsilane (TMS). Experiments were carried out in the temperature range 238−348 K. A 99.9% deuterated acetonitrile solution with addition of a small amount of TMS was used. Temperature variation was done by a JEOL variable temperature controller.

Relaxation Measurement. Longitudinal relaxation time (T_1) was measured by the inversion recovery technique, and it consists of the following train of pulse sequence:

$$(180°-\tau-90°-\mathrm{AQ}-D)_n$$

where AQ is the acquisition time and D is the delay time to allow equilibrium to be reached. The value of magnetization varies from $-M_z(\infty)$ when τ is 0 to $M_z(\infty)$ when τ is 5 times higher than T_1 and τ is the variable time delay between the two pulses. It is possible to relate the magnetization to the T_1 value by the expression

$$M_z(\tau) = M_z(\infty)[1 - 2\exp(-\tau/T_1)] \quad (1)$$

T_1 therefore can be calculated by least squares fit analysis of the experimental data as a function of τ.

Solid State Susceptibility Measurement. The solid state susceptibility measurement for **2** was performed in a quantum design SQUID susceptometer MPMS-5S in the temperature range 77−300 K with an applied field of 1 T. The data was corrected for the sample holder contribution and the diamagnetic contribution estimated through Pascal's constants.

Solution Susceptibility Measurement. Solution susceptibility of all of the complexes was measured by the modified Evans method.[44] Coaxial NMR tube was used with acetonitrile as an internal reference. The inner tube contains only acetonitrile while the outer tube contains both acetonitrile and binuclear copper(II) complex solution. The presence of copper(II) dimer in the outer tube makes the bulk susceptibility different from that of the inner tube. The CH_3 proton signals from acetonitrile in these two inner and outer tubes were recorded; the separation of the two signals ($\Delta\nu$) was monitored and is considered as a paramagnetic shift. Mass susceptibility (χ_p) is correlated to the above-mentioned paramagnetic shift as follows:

$$\chi_p = \chi_0 + 3000\Delta\nu/4\pi\nu_o cM \quad (2)$$

where c is the concentration of the solution in mol/L, M is the molecular weight of the complex, ν_o is the operating rf frequency of the spectrometer, and χ_0 is the susceptibility of pure solvent.

X-ray Crystallography. Crystal Data Collection and Refinement. Green crystals of $[(Cu_2(DMDAP)_2IPA)(OH)(H_2O)](ClO_4)_2$ (**2**) suitable for X-ray diffraction studies were obtained by slow evaporation of an aqueous solution of the complex. The diffraction intensities of an approximately 0.2 × 0.15 × 0.15 mm crystal were collected using an Enraf-Nonius CAD4 single-crystal diffractometer with Cu Kα radiation (1.541 84 Å). The cell parameters were obtained by the method of short vectors followed by least-squares refinement of 25 randomly chosen higher angle reflections. Stability of the crystal during data collection was checked by monitoring the intensities of two standard reflections after every 1 h of data collection. No significant variation of intensity could be noted. The intensity data were corrected for Lorentz, polarization, decay, and absorption (ψ-scan) effects using the computer program MolEN.[45] A total of 2642 reflections were collected in the range $8° > 2\theta < 136°$ of which 2443 reflections with $I > 2\sigma(I)$ were used for the structure determination. The structure was solved by direct methods using the computer program SHELXS-86[46] and refined using the program SHELXL-93.[47] All hydrogen atoms were fixed through the riding model procedure of SHELXL-93. The structure was refined by a full-matrix least-squares technique. The final residual factors were $R(F) = 0.0591$ and $R_w(I) = 0.1595$, respectively. The expressions for $R(F)$ and $R_w(I)$ are as follows:

$$R(F) = \sum||F_o| - |F_c||/\sum|F_o|$$

$$R_w(I) = [\sum[W[|F_o|^2 - |F_c|^2]]^2/\sum(W|F_o|^2)^2]^{1/2}$$

where

$$W = 1/[\sigma^2(F_o^2) + (0.066P)^2 + 2.6P]$$

$$P = (\mathrm{Max}(F_o^2,0) + 2F_c^2)/3$$

The final difference map was featureless. A summary of the crystal and diffraction data is given in Table 1, and atomic coordinates are given in Table 2.

Results and Discussion

Description of the Structure of $[(Cu_2(DMDAP)_2IPA)(OH)(H_2O)](ClO_4)_2$ (2). The solid state structures of **1** and **2** have

(43) Grzybowski, J. J.; Merrell, P. H.; Urbach, F. L. *Inorg. Chem.* **1978**, *17*, 3078.
(44) Sandip, K. S. *J. Magn. Reson.* **1989**, *82*, 169.
(45) Kay Fair, C. *MolEN Crystal structure analysis 1, 2 and 3*; Enraf-Nonius: Delft, 1990.
(46) Sheldrick, G. M. *SHELXS-86. A computer program for crystal structure determination*; University of Göttingen: Göttingen, 1985.
(47) Sheldrick, G. M. *SHELXL-93. A computer program for crystal structure determination*; University of Göttingen: Göttingen, 1993.

Table 1. Crystal Data and Structure Refinement for **2**

empirical formula	$C_{19}H_{32}Cl_2N_4Cu_2O_{11}$
fw	692.48
temp, K	293(2)
wavelength (λ), Å	1.541 84
cryst syst	monoclinic
space group	*Cc* (No. 9)
unit cell dimens	
a, Å	12.472(2)
b, Å	19.554(2)
c, Å	12.185(12)
α, deg	90
β, deg	107.48(9)
γ, deg	90
vol, Å^3	2834.4(5)
Z	4
density (calcd), g cm^{-3}	1.62
abs coeff (μ), cm^{-1}	41.19
$R(F_o)$	R1 = 0.0591
$R_w(F_o^2)$	wR2 = 0.1595

Table 2. Atomic Coordinates ($\times 10^4$) and Equivalent Isotropic Displacement Parameters (Å^2 $\times$ 10^3) for **2**[a]

atom	*x*	*y*	*z*	*U*(eq)
Cu(1)	906(1)	2369(1)	3039(1)	58(1)
Cu(2)	600(1)	1179(1)	4527(1)	63(1)
N(1)	2202(6)	2670(3)	2607(5)	55(1)
N(2)	−236(6)	2884(4)	1789(6)	64(2)
N(3)	1632(7)	435(4)	5207(6)	65(2)
N(4)	−827(7)	678(5)	4547(7)	79(2)
O(1)	1746(4)	1572(3)	3863(5)	57(1)
O(2)	−155(6)	1944(5)	3644(6)	82(2)
O(3)	777(11)	1795(6)	6152(8)	119(3)
Cl(1)	1539(7)	1686(3)	9117(4)	174(3)
O(4)	258(38)	1506(34)	8514(41)	465(37)
O(5)	1690(14)	1532(8)	10224(9)	145(5)
O(6)	1905(17)	1258(8)	8490(12)	164(6)
O(7)	1244(27)	2322(8)	8792(16)	204(9)
Cl(2)	6422(3)	1308(1)	393(2)	86(1)
O(8)	5314(25)	1019(16)	211(23)	265(15)
O(9)	6620(23)	1682(11)	1397(14)	212(10)
O(10)	6335(27)	1687(10)	−525(16)	236(12)
O(11)	7202(37)	848(22)	556(33)	446(33)
C(1)	2579(6)	1246(4)	3639(6)	51(2)
C(2)	3210(6)	1565(4)	2999(6)	52(2)
C(3)	4114(7)	1226(4)	2778(8)	61(2)
C(4)	4408(7)	565(5)	3164(9)	67(2)
C(5)	3822(8)	265(4)	3825(8)	67(2)
C(6)	2933(7)	590(4)	4082(7)	56(2)
C(7)	5368(12)	224(7)	2905(15)	104(4)
C(8)	3029(8)	2275(4)	2589(7)	58(2)
C(9)	2226(10)	3380(5)	2207(10)	79(2)
C(10)	1193(12)	3524(7)	1207(14)	107(5)
C(11)	126(13)	3523(9)	1395(17)	125(6)
C(12)	−612(13)	2374(6)	832(9)	95(4)
C(13)	−1277(11)	3034(8)	2124(14)	106(4)
C(14)	2459(9)	240(4)	4888(8)	67(2)
C(15)	1415(11)	48(6)	6163(8)	83(3)
C(16)	226(14)	−249(7)	5845(13)	108(4)
C(17)	−690(13)	282(7)	5622(12)	97(4)
C(18)	−1740(10)	1168(7)	4466(13)	99(4)
C(19)	−1190(12)	220(9)	3499(13)	110(5)

[a] *U*(eq) is defined as one-third of the trace of the orthogonalized $\mathbf{U}_{ij}$ tensor.

been determined X-ray crystallographically. The structural details of complex **1** have been reported elsewhere.[28b] The structural details of complex **2** are described here.

The ZORTEP[48] (30% probability thermal ellipsoid) representation of the $[(Cu_2(DMDAP)_2IPA)(OH)(H_2O)](ClO_4)_2$ (**2**) complex is shown in Figure 2a, and selected bond distances and bond angles around the Cu atoms are given in Table 3. The structure consists of two copper centers bridged by one phenoxy oxygen atom and one hydroxy oxygen atom with one

(48) Zsolnai, L.; Pritzkowm, H. *ORTEP program for Personal Computer*; University of Heidelberg: Heidelberg, Germany, 1994.

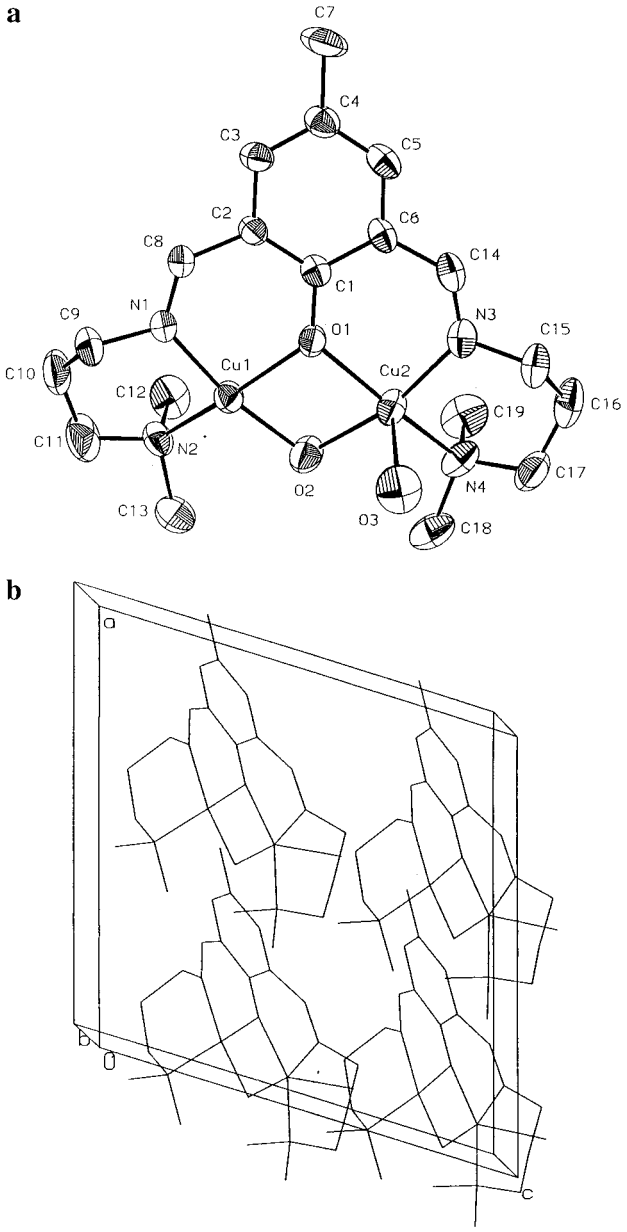

Figure 2. (a) ZORTEP representation for $[(Cu_2(DMDAP)_2IPA)(OH)(H_2O)](ClO_4)_2$ (**2**) with hydrogen and perchlorate atoms omitted (30% probability thermal ellipsoids). (b) Unit cell packing diagram for **2** along the *ac* plane.

Table 3. Selected Bond Distances (Å) and Angles (deg) for **2**

	Bond Distances		
Cu1−O2	1.889(7)	Cu2−O2	1.916(7)
Cu1−N1	1.936(7)	Cu2−N3	1.955(8)
Cu1−O1	1.976(5)	Cu2−O1	1.995(5)
Cu1−N2	2.014(7)	Cu2−N4	2.037(8)
Cu1−Cu2	3.043(2)	Cu2−O3	2.271(10)
	Bond Angles		
O2−Cu1−N1	168.3(3)	O2−Cu2−N3	165.7(3)
O2−Cu1−O1	77.3(3)	O2−Cu2−O1	76.3(3)
N1−Cu1−O1	91.1(2)	N3−Cu2−O1	89.9(3)
O2−Cu1−N2	95.5(3)	O2−Cu2−N4	95.6(4)
N1−Cu1−N2	95.8(3)	N3−Cu2−N4	95.9(4)
O1−Cu1−N2	157.7(3)	O1−Cu2−N4	157.5(3)
Cu1−O1−Cu2	100.1(2)	Cu1−O2−Cu4	106.2(3)

Table 4. Least-Squares Planes of **1**[a] and **2**[b]

Least-Squares Planes for **1**

equation of plane 1 (N1, N2, O1, O2)
$0.7909X + 0.3801Y - 0.4795Z - 2.3431 = 0$

atom	deviation from mean plane (Å)
N1	−0.1193
N2	0.1206
O1	−0.1415
O2	0.1404
Cu1	0.1744

$\chi^2 = 0.0$

equation of plane 2 (N3, N4, O1, O2)
$0.6511X + 0.5583Y - 0.5141Z - 3.7427 = 0$

atom	deviation from mean plane (Å)
N3	0.0431
N4	−0.0432
O	−0.0511
O2	0.0512
Cu2	0.0767

$\chi^2 = 0.0$

Least-Squares Planes for **2**

equation of plane 1 (N1, N2, O1, O2)
$0.4469X - 13.2871Y - 8.6485Z - 5.5832 = 0$

atom	deviation from mean plane (Å)
N1	−0.1196
N2	0.1958
O1	0.2290
O2	−0.1593
Cu1	−0.1519

$\chi^2 = 0.0$

equation of plane 2 (N3, N4, O1, O2)
$0.8270X - 9.8735Y - 10.2457Z - 5.5623 = 0$

atom	deviation from mean plane (Å)
N3	−0.0729
N4	0.1690
O1	0.1935
O2	−0.0987
Cu2	−0.1909

$\chi^2 = 0.0$

[a] Reference 28b. [b] This work.

imino nitrogen atom and one dimethylamino nitrogen atom completing the CuN_2O_2 plane. The Cu−Cu separation is 3.04 (2) Å, and the oxygen bridge angle from the azomethine unit Cu(1)−O(1)−Cu(2) and from the dimethyl unit Cu(1)−O(2)−Cu(2) are slightly different: 100.1(2)° and 106.2(3)°, respectively. The observed Cu−Cu distance and bond angles around Cu(1)−O(1)−Cu(2) and Cu(1)−O(2)−Cu(2) are comparable to those of the earlier reported binuclear Cu(II) complexes of this type.[27,28,49] Azomethine linkages N(1)−C(8) and N(3)−C(14) (mean 1.367 Å) are essentially double bond in character, whereas the dimethylamino C−N bond lengths N(2)−C(11) and N(4)−C(17) (mean 1.47 Å) can be described by a single-bond character. The least-squares plane calculations (Table 4) show that for Cu(1) donors O(1) and N(2) are displaced by 0.2290 and 0.1958 Å, respectively, on one side of the N_2O_2 mean plane, whereas donors O(2) and N(1) are displaced by −0.1533 and −0.1196 Å, respectively, on the other side of the mean plane. A similar situation exists around Cu(2). Donors O(1) and N(4) are displaced by 0.1935 and 0.1690 Å, respectively, on one side of the N_2O_2 mean plane, whereas donors O(2) and N(3) are displaced by −0.0987 and −0.0729 Å, respectively. It may, however, be noted that a deviation of donor atoms of Cu(1) from the mean plane is large in comparison to the plane surrounding Cu(2). The metal atom Cu(1) is significantly out of plane with a normal distance of −0.1519 Å from the mean plane. The deviation of metal atom Cu(2) from the mean plane, −0.1909 Å, is, however, large when compared to that of Cu(1). One water molecule occupies the axial position with a somewhat large contact of 2.274 (9) Å with Cu(2), which causes the metal center to displace toward water molecules. The geometry around Cu(2) is hence a distorted square pyramid. The perchlorate ion is weakly interacting with the Cu(1) ion, causing a small deviation of the Cu(1) ion from the mean plane toward the perchlorate group. This indicates the absence of bonding between Cu(1) and O(10) of the perchlorate group, the geometry around Cu(1) being distorted square planar.

The shortest Cu−Cu distance between two molecules is ∼7.6 Å, which could lead to weak interdimer exchange coupling. There are very few van der Waal contacts between the molecules. The interaction of molecules with anions and water molecules is responsible for crystal stability and packing forces. Figure 2b shows the packing diagram of molecules projected on the *ac* plane.

Magnetic Properties. Solid State Susceptibility. The room temperature solid state magnetic moments of the hydroxo-bridged complexes reported here range from 0.67 to 1.02 μ_B (Table 5) and indicate a high degree of antiferromagnetic interaction between the metal centers. These values are comparable to those obtained by Thompson,[49] Robson,[50] and Okawa and Kida[51] for similar systems.

The variable temperature magnetic studies on complex **2** were carried out in the temperature range 77−300 K. The variable temperature data was fitted to the Bleaney−Bowers[52] equation (eq 3), using the Heisenberg (isotropic) exchange Hamiltonian

$$\chi_M = \frac{Ng^2\beta^2}{3kT}\left[1 + \frac{1}{3}\exp\left(\frac{-2J}{kT}\right)\right]^{-1}(1-\rho) + \frac{Ng^2\beta^2}{4kT}\rho + N_\alpha \quad (3)$$

($H = -2JS_1 \cdot S_2$) for two interacting $S = {}^1/_2$ centers, where $-2J$ is the energy difference between the singlet and triplet states, χ_m is expressed per mole of copper atoms, N_α is the temperature independent paramagnetism, and ρ is the fraction of monomeric impurity. This procedure treats a complex as a ground state singlet with a low-lying triplet state. A simplex curve-fitting routine[53] was used to determine the parameters g and $-2J$. The best data fit to eq 3 gave $g = 2.13$ (±0.02), $-2J = 581$ (±6.0), $N_\alpha = 6.0 \times 10^{-5}$, $\rho = 0.038$, and least-squares error (R) = 2.13×10^{-4}. A plot of effective magnetic moment versus temperature is given in Figure 3. The observed and calculated magnetic moment μ_{eff} decreases from a value of 0.71 μ_B at 300 K to 0.35 μ_B at 77 K, indicating a strong intramolecular antiferromagnetic exchange interaction in this binuclear copper(II) system. A similar result was obtained for a dialkyl-substituted ethylenediamine of a binuclear copper(II) complex of this type.[54]

(49) Thompson, L. K.; Mandal, S. K.; Tandon, S. S.; Bridson, J. N.; Park, M. K. *Inorg. Chem.* **1996**, *35*, 3117.
(50) (a) Robson, R. *Aust. J. Chem.* **1970**, *23*, 2217. (b) Dickson, I. E.; Robson, R. *Inorg. Chem.* **1974**, *13*, 1301.
(51) (a) Okawa, H.; Kida, S. *Bull. Chem. Soc. Jpn.* **1971**, *44*, 1172. (b) Okawa, H.; Kida, S.; Muto, Y.; Tokii, T. *Bull. Chem. Soc. Jpn.* **1972**, *45*, 2480.
(52) Bleaney, B.; Bowers, K. *Proc. R. Soc. London, Sect. A* **1952**, *214*, 451.
(53) Chandramouli, G. V. R.; Balagopalakrishna, C.; Rajasekaran, M. V.; Manoharan, P. T. *Comput. Chem.* **1996**, *20*, 353.

Table 5. Magnetic Moments and Exchange Coupling Constants of **1**−**3** and, for Comparison, **4**

			μ_{eff}/μ_B		exchange coupling constant ($-2J$), cm^{-1}	
study no.	complex	solvent	solid	solution	solid	solution
1	$[(Cu_2(DAP)_2IPA)(OH)(H_2O)](ClO_4)_2 \cdot H_2O$ (**1**)	CD_3CN	0.67[a]	0.74[b]	∼600[c]	438 ± 5.63[b,d]
2	$[(Cu_2(DMDAP)_2IPA)(OH)(H_2O)](ClO_4)_2$ (**2**)	CD_3CN	0.71[b]	0.83[b]	581 ± 6.0[b]	398 ± 4.01[b,d]
3	$[(Cu_2(AEP)_2IPA)(OH)(H_2O)](ClO_4)_2$ (**3**)	CD_3CN	1.02[e]	0.84[b]	385[e]	396 ± 4.68[b,d]
4	$[Cu_2((ha)_2mpia)(OH)(H_2O)](ClO_4)_2$ (**4**)	CD_3OD	0.90[f]	0.70[f]	529[f]	

[a] From ref 42. [b] This work. [c] As derived from the μ_{eff} similarity of the compound in ref 31. [d] Calculated by solution susceptibility measurement using Bleany−Bowers equation (eq 4). [e] From ref 43. [f] From ref 27.

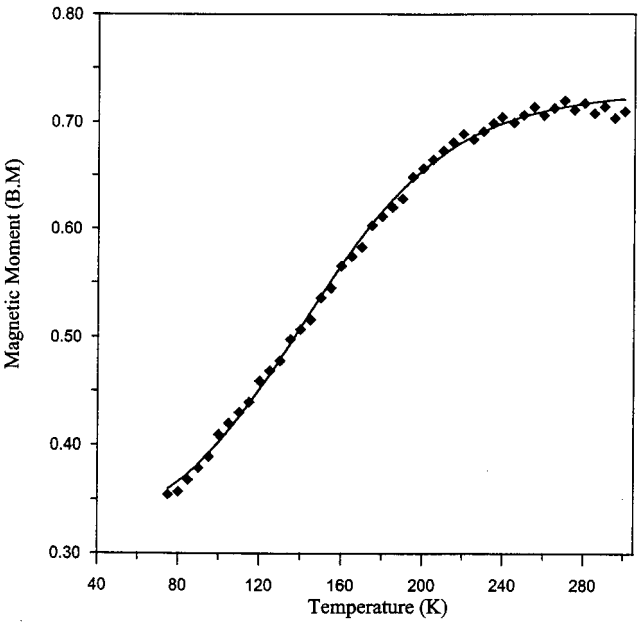

Figure 3. Plot of magnetic moment vs temperature for $[(Cu_2(DMDAP)_2IPA)(OH)(H_2O)](ClO_4)_2$ (**2**) in the solid state with ◆ representing the experimental data and the line representing the theoretical simulation using the expression in eq 3.

The variable temperature magnetic susceptibility measurement for complex **3** has already been reported.[43] The exchange coupling constant ($-2J$) for **3** obtained by using the Bleany−Bowers equation is 385 cm^{-1}. The corresponding magnetic moment obtained for this complex at 298 K is 1.02 μ_B, whereas the room temperature magnetic moments for complexes **1** and **2** are much less when compared to **3** (Table 5). The observed low magnetic moments in **1** and **2** indicate very strong antiferromagnetic exchange coupling operating in the dimers of these lattices. It may be noted that the azomethine linkage formed through DAP (**1**) and DMDAP (**2**) offers more flexibility in the metal−ligand linkages, which in turn leads to the augmentation of the Cu−O−Cu bridge angle relative to the less flexible configuration in **3**. Thus the stronger antiferromagnetic interactions expected for **1** and **2** are consistent with the observed moments.

The antiferromagnetic behavior of the binuclear complexes is attributed to spin−spin interaction occurring via the superexchange pathway provided by phenoxy bridging and hydroxy bridging, rather than a direct metal−metal interaction. The Cu−Cu distance in our binuclear systems is estimated to be ∼3.0 Å. This separation generally rules out any significant amount of direct Cu−Cu interaction. The observation that hydroxo bridges and phenoxo bridges provide more pathways for spin−spin interactions has been well characterized in the dimeric Cu(II) systems studied primarily by Hatfield[1] and Hodgson.[2]

Recent theoretical calculations[23] on exchange coupling of hydroxo-bridged binuclear Cu(II) complexes predict the relationship between the Cu−O−Cu bridge angle and the magnitude of the exchange coupling constant ($-2J$). When the bridge angle is 103°, the calculated exchange coupling constant is −543 cm^{-1}. However, they observed that small changes in the terminal ligands or the elimination of counterions could cause changes of the order of 50−60 cm^{-1}. So one can expect that complexes having a hydroxo bridge angle of ∼103° and 0.66 μ_B at 298 K can have an exchange coupling constant of ∼600 cm^{-1}.[31] In the case of complex **1**, the hydroxo bridge angle is 102.2° and the magnetic moment at room temperature is 0.67 μ_B, so the expected exchange coupling constant is ∼600 cm^{-1}. When the bridge angle increases, the exchange coupling constant is also expected to increase.[17,23] In the case of complex **2**, though the observed hydroxo bridge angle is higher (106.4°), the observed magnetic moment at room temperature is relatively high when compared to that of complex **1**. This is somewhat contrary to the expected trend, i.e., one should have expected larger antiferromagnetism in complex **2** rather than the complex **1**. The relatively high magnetic moment observed for **2** is due to the displacement of the Cu atom from the mean plane. Generally, the more planar is the geometry around the Cu(II) ion, the larger is the magnetic exchange interaction between the Cu(II) ions.[55] Least-squares plane (see Table 4) calculations show that complex **1** is more planar than complex **2**. So, the expected antiferromagnetism is more for complex **1** than for complex **2**. The bulky methyl group substituted at the N atom causes the large distortion of the Cu atom from the mean plane in **2**. Hence, this observed magnetic moment data is consistent with the structural data for these dimers.

Solution Susceptibility. We have measured the susceptibility of all three complexes in solution using the modified Evans method,[44] considered to be a sensitive experiment though our experiment is restricted only to a small range of temperature (unlike in the solid state) due to freezing and boiling point ranges of acetonitrile solvent as an internal standard. χ_p calculated from frequency shift as a function of temperature using eq 2 is then converted into molar susceptibility after the usual correction to χ_M is applied.[56] $\Delta\nu$, χ_p, and χ_M were obtained as a function of temperature. This molar susceptibility is then used to calculate the intradimer exchange coupling ($-2J$) using the Bleany−Bowers expression:[52]

$$\chi_M = \frac{Ng^2\beta^2}{3kT}\left[1 + \frac{1}{3}\exp\left(\frac{-2J}{kT}\right)\right]^{-1} \qquad (4)$$

A simplex curve-fitting routine[53] was used to determine the exchange coupling constant ($-2J$) of each set of magnetic

(54) Okawa, H.; Tokii, T.; Nonaka, Y.; Muto, Y.; Kida, S. *Bull. Chem. Soc. Jpn*. **1973**, *46*, 1462.

(55) (a) Okawa, H.; Honda, M.; Kida, S. *Chem. Lett*. **1972**, 1027. (b) Muto, Y.; Kato, M.; Jonassen, H. B.; Cusachs, L. J. *Bull. Chem. Soc. Jpn*. **1969**, *42*, 417. (c) Kato, M.; Muto, Y.; Jonassen, K.; Imai, K.; Katsuki, K.; Ikegami, S. *Bull. Chem. Soc. Jpn*. **1969**, *42*, 2555.

(56) Carlin, R. L. In *Magnetochemistry*; Springer-Verlag: New York, 1986; p 3.

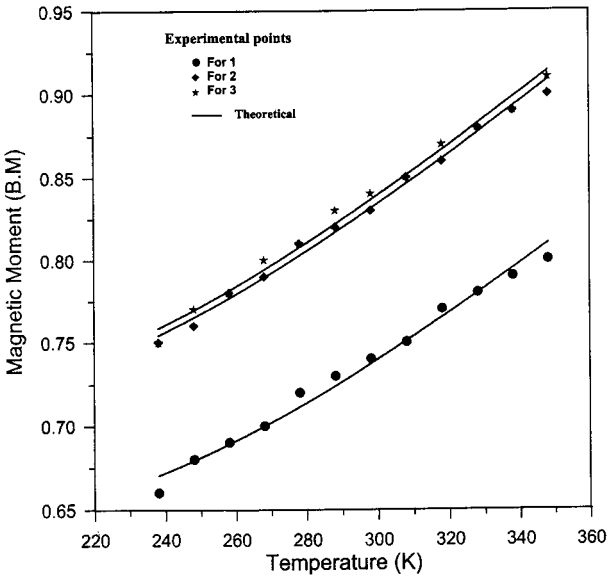

Figure 4. Plot of magnetic moment vs temperature for **1**, **2**, and **3** in solution using the expression given in eq 4 with ● for **1**, ◆ for **2**, and ★ for **3** representing experimental data points and the solid lines representing the best fit lines obtained.

susceptibility data for all three complexes. Figure 4 illustrates the type of "best fits" obtained for **1**−**3**. The $-2J$ values are found to be in the range 438−396 cm^{-1} (Table 5) for the three complexes reported here. The magnetic moments obtained by this method are in general comparable to the solid state magnetic moment (Table 5). These data indicate that the Cu(II) ions in all three complexes are strongly antiferromagnetically coupled in acetonitrile solution because of the retention of the macromolecular structure within the dimer moiety.

The slight differences monitored in the solution are due to coordination by solvent molecules and loosening of solid state packing accompanied by loss of interdimer interactions.[27]

The NMR Spectra and Isotropic Shift. The representative proton NMR spectra of complexes **1**−**3** at room temperature are shown in Figure 5a−c. All three binuclear complexes exhibit relatively sharp hyperfine shifted signals spanning from 82 to −30 ppm for **1**, from 97 to −41 ppm for **2**, and from 113 to −43 ppm for **3**. Spectra of **1**−**3** were monitored by variable temperature measurements (−35 to 75 °C). Though there are many peaks, we are able to easily identify the change in chemical shift as a function of temperature for five to six protons as shown in Table 6. They are all quite sensitive to temperature; the shift as a function of temperature for the OH proton (A) in **1** is 50 ppm, in **2** is 42 ppm, and in **3** is 34 ppm in the above said temperature region (see Figure 6). The shift of the $=N-CH_2$ proton (E) in **1** is 17 ppm, in **2** is 17 ppm, and in **3** is 13 ppm (see Figure 6). All other protons reveal a much lower shift of around 5 ppm over the studied temperature region. A plot of chemical shift vs $1/T$ is given in Figure 6 only for protons A and E of **1**−**3** which have shown very large shifts (see Supporting Information for the plot of chemical shift vs $1/T$ for all protons of **1**−**3**). The other protons do not show such drastic variations. It must be noted here that the NMR spectra of the pure ligand in the same solvent do not show observable shifts with temperature.[28a,57,58] Moreover, all three complexes follow anti-Curie behavior, i.e., shift increases as the temperature

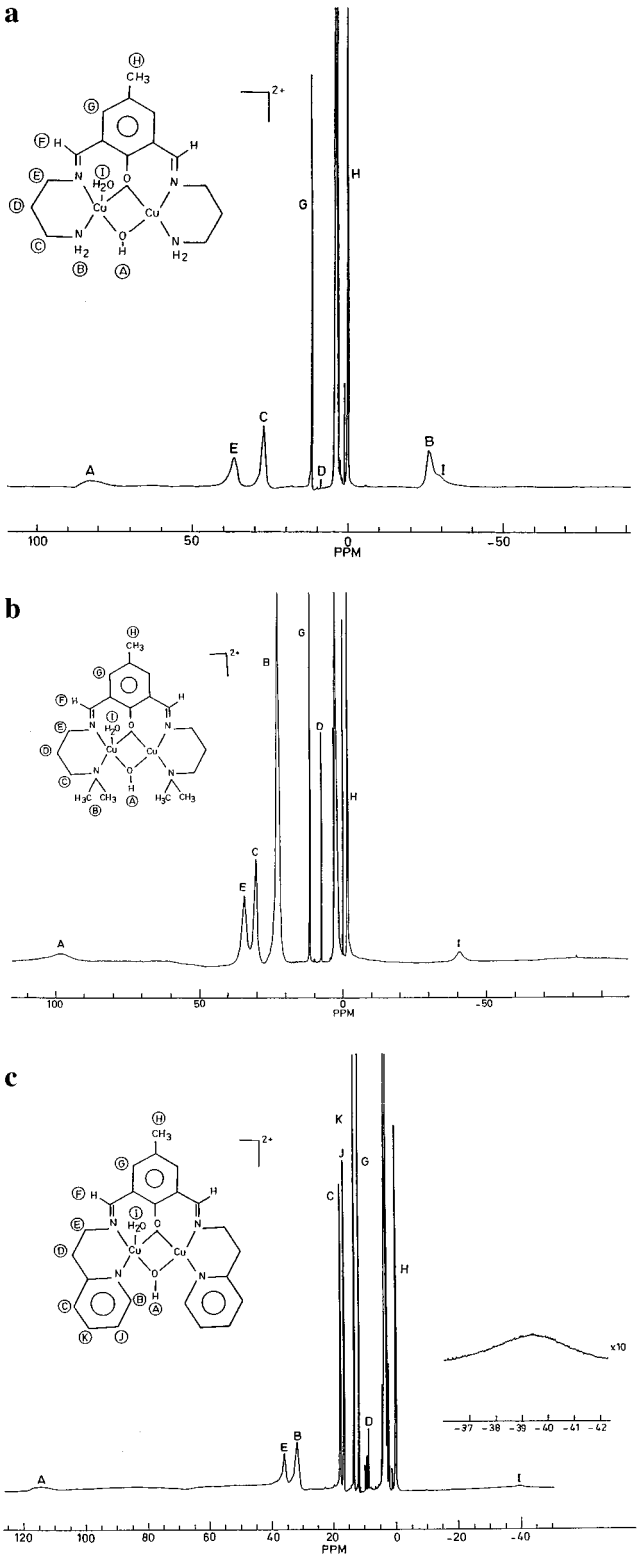

Figure 5. (a) ^1H NMR spectrum for **1** in CD_3CN solution at room temperature. (b) ^1H NMR spectrum for **2** in CD_3CN solution at room temperature. (c) ^1H NMR spectrum for **3** in CD_3CN solution at room temperature.

increases. It has been recently shown by Holz et al.[31] that the antiferromagnetically coupled dicopper(II) systems having a $-2J$ value of ∼250 cm^{-1} will follow Curie behavior, whereas those with a $-2J$ value of ∼350 cm^{-1} may follow anti-Curie or non-Curie behavior. The $-2J$ value for complexes **1**, **2**, and **3** are ∼600, 581, and 385 cm^{-1}. Hence it is not surprising that these complexes follow anti-Curie behavior.

(57) La Mar, G. N.; Horrocks, W. D.; Holm, R. H. *NMR of paramagnetic molecules: Prinicples and applications*; Academic Press: New York, 1973; Chapter 4.
(58) Kitagawa, S.; Munakata, M.; Yonezawa, M. *Kinki Univ. J.* **1985**, 61.

Table 6. Peak Positions, T_1 and T_2 Values, Proximity of Hydrogens to Cu, and Assignments for **1**−**3** at Room Temperature (25 °C)

labeling	assignment	chem shift,[a] ppm	T_1,[b] ms	T_2,[c] Hz	R_{Cu-H}, Å X-ray	R_{Cu-H}, Å soln[d]
		Complex **1**				
A	O−H	82.26				
B	NH_2	−27.31	∼1	907	3.39	2.96
C	H_2N-CH_2	25.59	8.00	580	4.99	4.19
D	$-CH_2$	7.5				
E	$=N-CH_2$	34.92	7.54	1500	4.86	4.15
F	CH=N					
G	Ar−H	10.46	51.13*	20	5.70	
H	CH_3	−0.48				
I	H_2O	−30				
		Complex **2**				
A	O−H	97.24				
B	$N-(CH_3)_2$	22.56	4.511	360	3.92	3.80
C	$(CH_3)_2-N-CH_2$	30.24	6.821	486	4.90	4.06
D	$-CH_2$	7.56				
E	$=N-CH_2$	34.09	5.910	789	4.81	3.97
F	CH=N					
G	Ar−H	11.50	42.35*	15	5.51	
H	CH_3	−1.6	12.45	41		
I	H_2O	−41.25				
		Complex **3**				
A	O−H	113.76				
B	PyN=CH (α)	31.30				
C	Py β-H	16.77				
D	$-CH_2$	7.55				
E	$=N-CH_2$	35.52				
F	CH=N					
G	Ar−H	10.84				
H	CH_3	−1.75				
I	H_2O	−43.20				
J	Py β-H	15.75				
K	Py γ-H	12.35				

[a] All shifts are in ppm related to TMS. [b] T_1 values are obtained using inversion recovery method. [c] The line widths are full width at half-maximum. [d] In solution, calculated $R_{Cu-H} = R_{ref}(T_{1i}/T_{1ref})^{1/6}$, where R_{ref} and T_{ref} are reference (*) values.

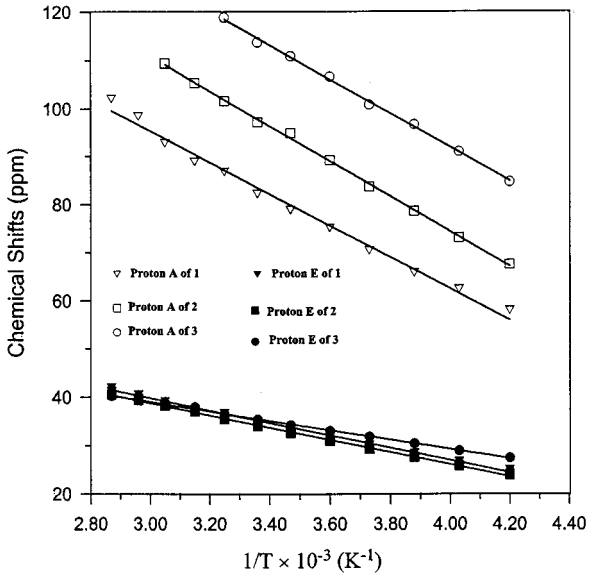

Figure 6. Plot of chemical shift vs T^{-1} only for protons A and E for dimers **1**, **2**, and **3**.

Signal Assignment. $[(Cu_2(DAP)_2IPA)(OH)(H_2O)](ClO_4)_2 \cdot H_2O$ (1). We have observed the change in chemical shift as a function of temperature for protons A, B, C, E, G, and I of **1** in CD_3CN (Figure 7a (protons B, C, E, and I are shown) and Table 6). Signals have been assigned using[30] (i) proton longitudinal relaxation time (T_1), (ii) line width that correlates with through-bond delocalization, and (iii) signal intensity. The first point refers to the general observation that the majority of protons close to copper will have short T_1s in the narrow range 5−10 ms (in the case of complex **1**) with broader line widths (shorter T_2 values), and those in the periphery will have longer T_1s of ∼50 ms (in the case of complex **1**) and hence narrow line widths. The assumption is based on the fact that the protons closer to the copper centers experience a stronger paramagnetic effect and hence shorter T_1s and larger shifts. Another observation is that there is a good correlation between the solution determined Cu−H distances using[29c] relative T_1 values and the range found in the structure (Table 6). In fact on the basis of these data one can assign the observed signals that are closer to copper without any difficulty, as they are not accessible to 2D techniques because of their very short relaxation times. On the basis of the above three points the signals C, D, E, G, and H were assigned; these are consistent with the earlier reports on binuclear copper(II) complexes having a similar environment.[27,28a] Signals A, B, and I are the only remaining unassigned signals in the proton NMR spectrum of **1**. Upon the addition of a small amount of D_2O, all these proton signals disappear, indicating that these protons are all exchangeable protons. Signal B was assigned as an NH_2 proton, because comparison of the spectrum of **1** with that of a related complex **2** where the amino hydrogens are replaced by methyl groups gives the opposite shift behavior (see Figure 7b, proton B) as expected due to opposite spin density mechanism as a result of spin polarization.[59−61] Signal A was assigned to the OH proton on the basis of the unpaired electron being present in the $d_{x^2-y^2}$ orbital. This would give a predominant σ mechanism[22,27,28a] for superexchange causing a large downfield shift for the OH proton. The remaining signal I is assigned as an axially coordinated water proton signal. In this case a spin polarization mechanism gives an upfield shift. The aldimine proton CH=N (F) could not be detected because of its significant line broadening.[27]

It may be seen that protons A, C, and E undergo a downfield shift with an increase in temperature while the other two protons B and I demonstrate an upfield shift. The line width of A, C, and E increases with an increase in temperature. It can be seen in antiferromagnetically coupled dicopper(II) systems that the population distribution in the $S = 0$ and $S = 1$ states will vary with temperature and consequently the additional field due to unpaired electrons (from the $S = 1$ state) at various nuclei causes simultaneous line broadening and shift. As was the case with the earlier published work,[27] the $-CH_2$ group protons adjacent to the coordinated nitrogen ligands seem to broaden quite considerably due to a quadrupole effect from ^{14}N, i.e., protons C and E in our case. They also seem to suffer the maximum temperature dependent shift next to OH and NH_2, indicating the dominance of σ bond effects in exchange coupling. In other words the superexchange occurs via the σ moiety. The earlier theoretical calculations of exchange coupling constants[22] indicate that σ is the dominant route for exchange coupling.

$[(Cu_2(DMDAP)_2IPA)(OH)(H_2O)](ClO_4)_2$ (2). The variable temperature spectrum of **2** in CD_3CN solution is given in Figure 7b (protons A, B, C, E, and I are shown). This figure shows a spectral pattern similar to that of **1** except for the signal observed at 23 ppm (Figure 7b (proton B), Table 6). Signal assignments

(59) Eaton, D. R.; Josey, A. D.; Phillips, W. D.; Benson, R. E. *J. Chem. Phys.* **1962**, *37*, 347.
(60) La Mar, G. N.; Horrocks, W. D.; Allen, L. C. *J. Chem. Phys.* **1964**, *41*, 2126.
(61) Forman, A.; Murrell, J. N.; Orgel, L. E. *J. Chem. Phys.* **1959**, *31*, 1129.

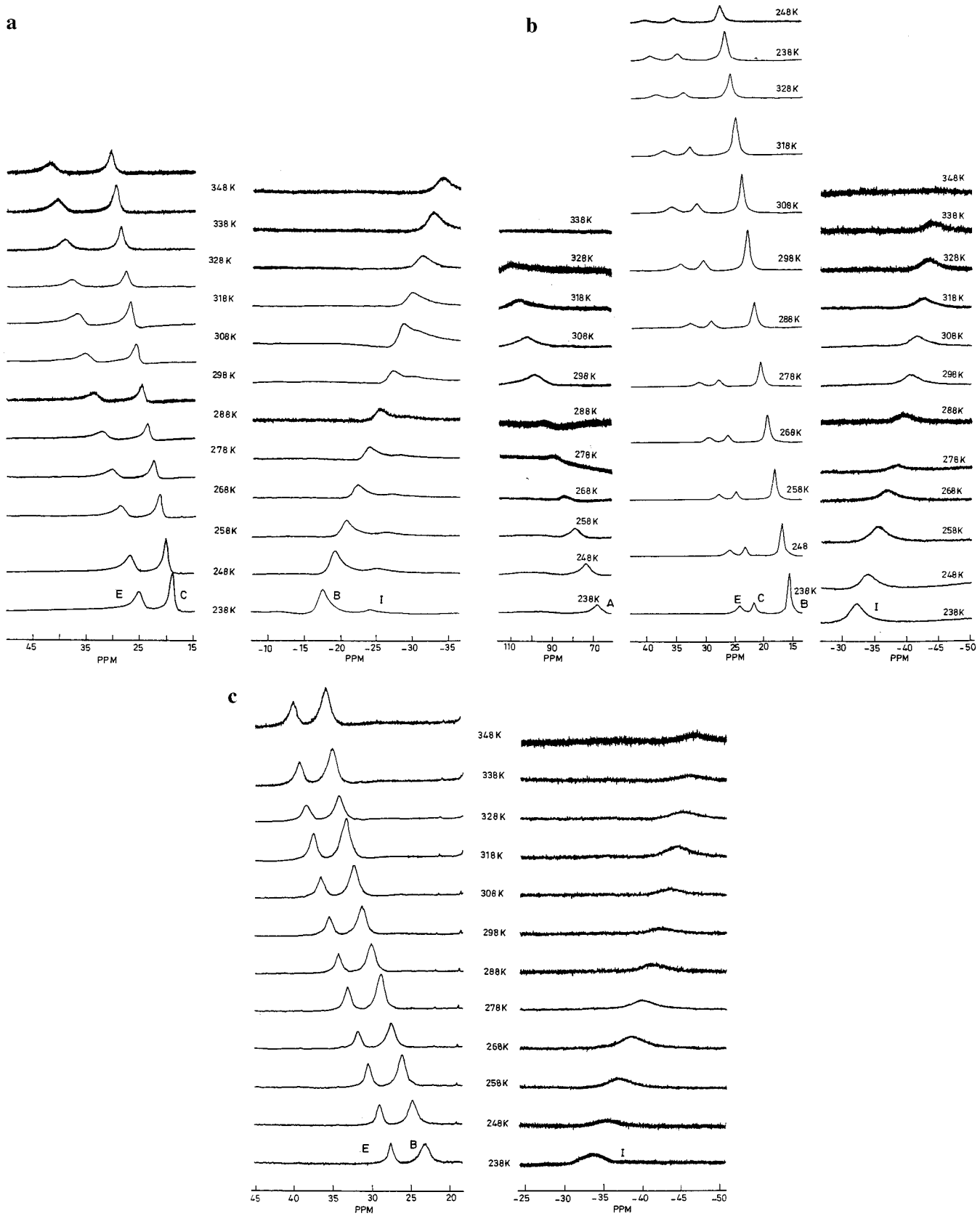

Figure 7. (a) Variable temperature ^{1}H NMR spectra of E, C, B, and I protons of **1** in CD_3CN solution. (b) Variable temperature ^{1}H NMR spectra of A, E, C, B, and I protons of **2** in CD_3CN solution. (c) Variable temperature ^{1}H NMR spectra of E, B, and I protons of **3** in CD_3CN solution.

for protons C, D, E, G, and H were made on the basis of **1**. The peak observed at 23 ppm (B) corresponds to $(CH_3)_2-N$. This is confirmed by signal intensity as well as the opposite shift behavior observed for complex **1** where methyl groups are replaced by hydrogen atoms. This is due to the fact that methyl substituents always produce shifts of opposite sign to that of hydrogen atom.[59−61] Signals A (97 ppm) and I (−41 ppm) at room temperature are the only remaining unassigned signals in the ^{1}H NMR spectrum of **2**. These signals can be assigned as OH (A) and axially coordinated water protons (I), since the

Table 7. Hyperfine Coupling Constants (A) for Different Protons and Exchange Coupling Constant ($-2J$) Obtained from $\Delta\delta_{iso}$ Using Eq 6 for **1**−**3**

proton type	$-2J$, cm^{-1}	A, Hz
	Complex **1**	
O−H	390 ± 4.1	153, 995
=N−CH_2	379 ± 2.5	59, 5577
H_2N−CH_2	372 ± 2.5	41, 0758
NH_2	412 ± 2.1	−60, 8182
	Complex **2**	
O−H	381 ± 1.7	167, 413
=N−CH_2	381 ± 1.4	58, 7110
$(CH_3)_2$−N−CH_2	375 ± 1.1	49, 6045
$(CH_3)_2$−N	392 ± 1.8	42, 3937
H_2O	340 ± 1.7	−51, 4036
	Complex **3**	
O−H	356 ± 2.0	161, 314
=N−CH_2	351 ± 2.4	48, 4219
PyN=CH	364 ± 2.1	47, 3117
H_2O	336 ± 2.3	−52, 1215

addition of a small amount of D_2O causes these signals to disappear. Moreover, as in the case of **1**, here again spin is transmitted predominantly via a σ mechanism. It is to be emphasized that the observed chemical shift range slightly differs from that of **1**. This is supported also by the T_1 values.

[(Cu_2(AEP)$_2$IPA)(OH)(H_2O)](ClO_4)$_2$ (3). The variable temperature spectrum of **3** in CD_3CN solution is given in Figure 7c (protons B, E, and I are shown). Several of the isotropically shifted ^{1}H NMR signals observed for **3** can be assigned on the basis of signal intensity and of T_1 values. Signals D, E, G, and H (Table 6) are assigned on the basis of **1** and **2**. Signals B, C, J, and K (Table 6) were assigned on the basis of earlier reported similar systems.[29c] The signals observed at 113 ppm (A) and −43 ppm (I) are the only unassigned signals for this complex. These signals disappeared when a drop of D_2O was added, indicating that these signals are exchangeable proton signals. As was said earlier, σ is the dominant route for exchange coupling of these systems and the closeness of the oxygen atom of the hydroxy group (A) to the metal center leads to a direct delocalization of the unpaired electron from the cupric ion, giving a large downfield shift. However, the weak axially coordinated water proton (metal−oxygen bond is long) (I) gives an upfield shift due to a spin polarization mechanism.

Calculation of Exchange Coupling Constant in Solution Using Chemical Shift. In solution the magnetism of the exchange-coupled system can be explained by the simple Heisenberg Hamiltonian

$$H = -2JS_1 \cdot S_2 \tag{5}$$

with $S_1 = S_2 = {}^1/_2$; the temperature variation of chemical shifts could be used to calculate the exchange coupling using the expression[27]

$$\Delta\delta_{iso} = \frac{-g\beta A}{(\gamma/2\pi)kT}\left[3 + \exp\left(\frac{-2J}{kT}\right)\right]^{-1} \tag{6}$$

where A is the hyperfine coupling from the proton under reference, γ is the magnetogyric ratio, and $-2J$ is the exchange coupling constant.

A computer program[53] was constructed to fit experimental values of $\Delta\delta_{iso}$ and T for parameters A and $-2J$ by a least-squares method. The value of g in the calculated expression for $\Delta\delta_{iso}$ was taken as 2.0023. The best fit values of A and $-2J$ for all three complexes (**1**, **2**, and **3**) are given in Table 7. The agreement factor or least-squares error (R) is calculated using

$$R = \frac{\sum(\Delta\delta_{iso}^{obsd} - \Delta\delta_{iso}^{calcd})^2}{\sum(\Delta\delta_{iso}^{obsd})^2} \tag{7}$$

The fitting was found to be excellent in all cases with the least error value of the order of 10^{-4} for R.

Table 8. Exchange Coupling Constants for the Intradimer Interactions Derived from Various Experimental and Theoretical Studies

complex	method	$-2J$ (cm^{-1})
1	solid state	∼600[a]
	theoretical calculation	472[b]
	solution state	
	(a) susceptibility measurement	438 ± 5.6[c]
	(b) isotropic chemical shift measurement	388 ± 17[c]
2	solid state	581[c]
	theoretical calculation	567[b]
	solution state	
	(a) susceptibility measurement	398 ± 4.0[c]
	(b) isotropic chemical shift measurement	374 ± 20[c]
3	solid state	385[d]
	theoretical calculation	416[b]
	solution state	
	(a) susceptibility measurement	396 ± 4.7[c]
	(b) isotropic chemical shift measurement	352 ± 12[c]

[a] From ref 31. [b] From ref 23b. [c] This work. [d] From ref 43.

Figure 8a shows the experimental points and the lines for corresponding least-squares fit (using eq 6) for protons A, E, C, and B (Table 6) in the case of complex **1**. It is noteworthy to mention that $-2J$ values calculated for these protons range between 372 and 412 cm^{-1} (Table 7). This small uncertainty in $-2J$ arises chiefly owing to the errors arising from the small variations in the observed chemical shift over the limited temperature range used. However, the hyperfine coupling constant is different for different protons (Table 7) as expected. Similar results were obtained for binuclear iron(III) complexes[62] and binuclear copper(II) complexes.[28a] A comment on the origin of different hyperfine couplings on protons will be in order. This electron−nucleus hyperfine interaction constant (A) can have a contribution from either contact or dipolar interaction or both. It is well-known that the magnetic anisotropy giving rise to the dipolar or pseudocontact contribution is usually very small for Cu(II) systems.[63] In these cases contact shift is the predominant one. The contact shift due to spin transmitted through σ bonds predicts positive spin densities at protons A, E, and C and negative spin densities at protons B and I as it is assigned now and hence the hyperfine coupling constants with their respective signs. Also the magnitude of the spin densities due to contact shift will steadily decrease as a function of bonds away from the first coordination sphere of the metal atom.

Figure 8b shows a similar plot of experimental points and the lines for the corresponding least-squares fit (using eq 6) for protons A, E, C, and B (Table 6) in the case of complex **2**. The $-2J$ values calculated for these protons with a range of 375−392 cm^{-1} and the corresponding hyperfine coupling constant (A) values are given in Table 7. A comparison of the $2J$ value of **2** with **1** indicates that the antiferromagnetism is slightly reduced in **2** (vide supra).

Figure 8c shows a similar plot of experimental points and the lines for the corresponding least-squares fit (using eq 6) for protons A, E, and B (Table 6) in the case of complex **3**. The

(62) Boyd, P. D. W.; Murray, K. S. *J. Chem. Soc. A* **1971**, 2711.
(63) Esperson, W. G.; Martin, R. B. *J. Am. Chem. Soc*. **1976**, *98*, 40.

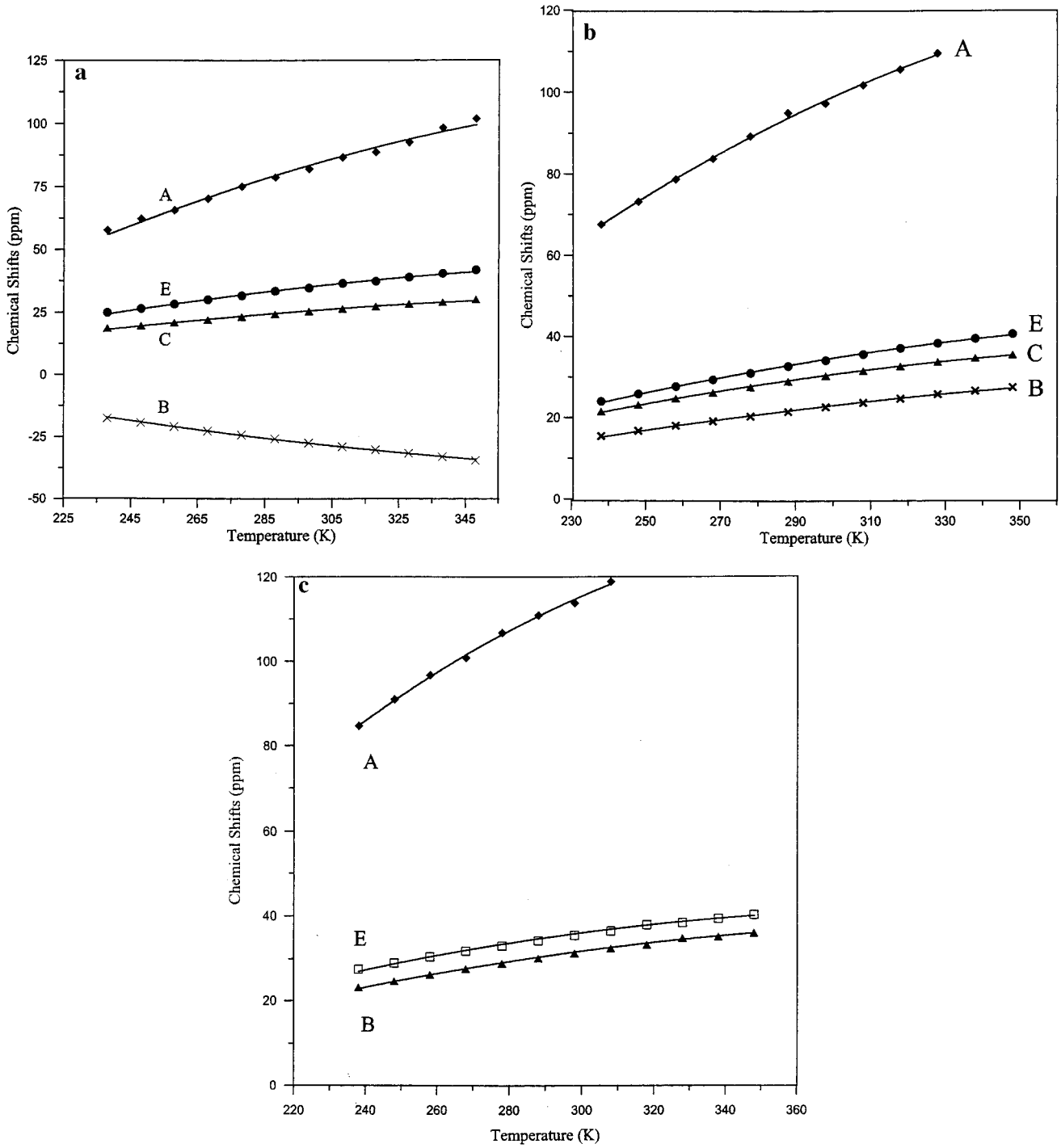

Figure 8. (a) Plot of chemical shift vs temperature for **1** with ◆, ●, ▲, and × representing experimental data points for protons A, E, C, and B, and the solid lines representing the best fits obtained from eq 6. (b) Plot of chemical shift vs temperature for **2** with ◆, ●, ▲, and × representing experimental data points for protons A, E, C, and B, and the solid lines representing the best fits obtained using eq 6. (c) Plot of chemical shift vs temperature for **3** with ◆, □, and ▲ representing experimental data points for protons A, E, and B, and the solid lines representing the best fits obtained with the use of eq 6.

$-2J$ values calculated for these protons in the range 316−356 cm^{-1} and the corresponding hyperfine coupling constant (A) values are given in Table 7. If the $-2J$ values of **1** and **2** are compared with those of **3**, there is a small reduction in the $-2J$ value of **3**, indicating that the antiferromagnetism is further reduced in **3** (vide supra).

At this point it is interesting to compare the results on exchange coupling obtained from different methods as summarized in Table 8. The diferences in $-2J$ between solid (by SQUID) and solution (by NMR) can be substantial in some cases and minor in other cases mainly due to structural packing and intermolecular interactions in solids getting totally or partially altered in solution. Such observations are very well-known.[27,28a,34a] Moreover, a solvent perturbation can change the bridge angle (M−O−M), which can alter the $-2J$ value to a great extent.[34a] In other cases, such perturbation can be small. However, all these data (Table 8) indicate that these complexes are strongly antiferromagnetically coupled in both solid and solution states.

We also attempt to give a magnetostructural correlation for eight dimers (Table 9) including the presently reported ones

Table 9. Magnetic and Structural Parameters (Bond Distances, Å; Bond Angles, deg) for Binuclear Cu(II) Complexes[a]

study no.	compound	Cu−Cu, Å	Cu−O−Cu, deg	$-2J$, cm^{-1}	ref
1	$[(Cu_2(ha)_2MPIA)(OH)(H_2O)](ClO_4)_2$	3.011	102.94	529	27
2	$[Cu_2(C_{36}H_{32}N_4O_4)]\cdot CH_3CN\cdot H_2O$	3.018	101.5	300	28a
3	$[(Cu_2(DAP)_2IPA)(OH)(H_2O)](ClO_4)_2\cdot H_2O$	3.010	102.2	600	28b
4	$[(Cu_2(AEP)_2IPA)(OH)(H_2O)](ClO_4)_2$			385	43
5	$[(Cu_2(L1)(H_2O)_2]F_2(CH_3OH)_2$	3.12	103.6	784	48
6	$[FSal(=NenNR_2)_2Cu_2(OH)](ClO_4)_2$			330	53
7	$[Cu_2(N_6O)(OH)][BF_4]$	3.05	103.6	410 ± 10	65
8	$[(Cu_2(DMDAP)_2IPA)(OH)(H_2O)](ClO_4)_2$	3.04	106.4	581 ± 6	this work

[a] ha = histamine; MPIA, IPA = 2-hydroxy-5-methylisophthalaldehyde; DAP = 1,3-diaminopropane; L1 = [2 + 2] condensation of 2,6-diformyl-4-methylphenol with 1,3-diaminopropane; $FSal(=NenNR_2)_2$ = Schiff base prepared from 2,6-diformyl-4-methylphenol and *N*,*N*-dialkylethylenediamine (alkyl = methyl); AEP = 2-(2-aminoethyl)pyridine; DMDAP = *N*,*N*-dimethyl-1,3-diaminopropane.

and some from our earlier work.[28a,b] It seems that all of these dimers are mostly hydroxy and phenoxy bridged and, having $Cu_2N_4O_2$ type chromophores with Cu−Cu bond distances of ∼3.05 ± 0.05 Å and a Cu−O−Cu bridge angle of 103° ± 2°, are strongly coupled, to the extent of $-2J$ being 300−700 cm^{-1}, amounting to an average of ∼490 cm^{-1}. The variation must be due to other influences such as differing π bonding effect induced by solid state packing creating distortion from planarity in addition to the common σ bonding effect as well as interdimer interactions.

This also draws support from the $-2J$ value of 438−396 cm^{-1} for relaxed dimers of **1**−**3** in solution, where the additional interactions are absent.

Relaxation Mechanism. We have investigated the NMR proton relaxation in two (**1** and **2**) of the three exchange-coupled systems reported here. In principle the relaxation measurements provides a wealth of information both on the extent of the interaction between the resonating nuclei and the paramagnetic center and on the time dependence of the parameters associated with the interaction. The time dependent phenomena associated with electron−nucleus interactions are related to the relaxation process of the electrons themselves, to the tumbling of the molecular system, and to the lifetime of different chemical situations, if they are available for the resonating nucleus. The T_1 values are measured by using an inversion recovery method.

In the case of dicopper(II) systems **1** and **2** the T_1 values are mainly due to dipolar relaxation mechanisms, as evidenced by the good agreement between the crystallographic distances and those calculated on the basis of a $1/r^6$ dependence (Table 6). Therefore, we can estimate the correlation time τ_c for these dimers. Hence we are tempted to use the recent formulations of Murthy et al.[30] to calculate τ_c and correlate it to τ_s and/or τ_r in view of their successful interpretation. On the other hand, in their systems, $|2J| \ll kT$, justifying the relaxation mechanism to be mainly of dipolar origin. In our case, since $|2J| \gg kT$, the relaxation should be of exchange modulated dipolar mechanism. This $|2J|$ should find its expression in any equation related to T_1, and hence it is more apt that we use the formulation of Bertini et al.[33b,64] for strongly exchange coupled systems.

The equations for proton longitudinal and transverse relaxation rate enhancements due to dipolar and contact coupling to an exchange-coupled system can be represented by

$$T_{1M}^{-1} = \frac{2}{15}\left(\frac{\mu_0}{4\pi}\right)^2 \frac{\gamma_I^2 g_e^2 \mu_B^2}{r^6} \sum_i \left[C_i^2 S_i'(S_i'+1)(2S_i'+1) \times \exp(-E_i/kT)\left(\frac{7\tau_c}{1+\omega_s^2\tau_c^2} + \frac{3\tau_c}{1+\omega_I^2\tau_c^2}\right)\right] \Big/ [\sum_i [(2S_i'+1) \times \exp(-E_i/kT)]] \quad (8)$$

$$T_{2M}^{-1} = \frac{1}{15}\left(\frac{\mu_0}{4\pi}\right)^2 \frac{\gamma_I^2 g_e^2 \mu_B^2}{r^6} \sum_i \left[C_i^2 S_i'(S_i'+1)(2S_i'+1) \times \exp(-E_i/kT)\left(4\tau_c + \frac{13\tau_c}{1+\omega_s^2\tau_c^2} + \frac{3\tau_c}{1+\omega_I^2\tau_c^2}\right)\right] \Big/ [\sum_i [(2S_i'+1) \exp(-E_i/kT)]] \quad (9)$$

$$T_{1M}^{-1} = \frac{2}{3}\frac{a^2}{\hbar^2} \sum_i \left(C_i^2 S_i'(S_i'+1)(2S_i'+1) \times \exp(-E_i/kT)\frac{\tau_s}{1+\omega_s^2\tau_s^2}\right) \Big/ [\sum_i [(2S_i'+1) \exp(-E_i/kT)]] \quad (10)$$

$$T_{2M}^{-1} = \frac{1}{3}\frac{a^2}{\hbar^2} \sum_i \left[C_i^2 S_i'(S_i'+1)(2S_i'+1) \times \exp(-E_i/kT)\frac{\tau_s}{1+\omega_s^2\tau_s^2}\right] \Big/ [\sum_i [(2S_i'+1) \exp(-E_i/kT)]] \quad (11)$$

In the case of dicopper(II) systems,

$$S_i' = 0, 1; \quad C_i = {}^1/_2; \quad E_i = 0, 1$$

After substituting these values, eqs 8−11 reduce to

$$T_{1M}^{-1} = \frac{2}{15}\left(\frac{\mu_0}{4\pi}\right)^2 \frac{\gamma_I^2 g_e^2 \mu_B^2}{r^6}\left[\frac{7\tau_c}{1+\omega_s^2\tau_c^2} + \frac{3\tau_c}{1+\omega_I^2\tau_c^2}\right] \Big/ \left[2 + \frac{2}{3}\exp(-2J/kT)\right] \quad (12)$$

$$T_{2M}^{-1} = \frac{1}{15}\left(\frac{\mu_0}{4\pi}\right)^2 \frac{\gamma_I^2 g_e^2 \mu_B^2}{r^6}\left[4\tau_c + \frac{13\tau_c}{1+\omega_s^2\tau_c^2} + \frac{3\tau_c}{1+\omega_I^2\tau_c^2}\right] \Big/ \left[2 + \frac{2}{3}\exp(-2J/kT)\right] \quad (13)$$

$$T_{1M}^{-1} = \frac{2}{3}\frac{a^2}{\hbar^2}\frac{\tau_s}{1+\omega_s^2\tau_s^2} \Big/ \left[2 + \frac{2}{3}\exp(-2J/kT)\right] \quad (14)$$

$$T_{2M}^{-1} = \frac{1}{3}\frac{a^2}{\hbar^2}\frac{\tau_s}{1+\omega_s^2\tau_s^2} \Big/ \left[2 + \frac{2}{3}\exp(-2J/kT)\right] \quad (15)$$

For proton, the value for the constant[40] $(2/15)(\mu_0/4\pi)^2\gamma_I^2 g_e^2 \mu_B^2$ is 3.29×10^{-44} m^6 s^{-2}; r is the distance from the metal center to

the proton; and ω_s and ω_I are the transition frequencies for the electron and proton, respectively. Equation 12 serves as the basis for interpreting T_1 values in exchange-coupled systems where $|2J| \gg kT$ and where dipolar relaxation is the dominant effect.

The correlation time τ_c in eq 8 is the reciprocal of rate constant τ_c^{-1}. This overall rate τ_c^{-1} is the sum of rates for three different processes,[33a]

$$\tau_c^{-1} = \tau_s^{-1} + \tau_r^{-1} + \tau_m^{-1} \tag{16}$$

where τ_s^{-1} is the electron spin relaxation rate, τ_r^{-1} is the rotational correlation rate, and τ_m^{-1} is the chemical exchange rate. In the case of systems reported here τ_m is of no consequence.

So we have estimated τ_c by using eq 12. Average τ_c values of around 2.14×10^{-10} s and 1.86×10^{-10} s are obtained for complexes **1** and **2**, respectively. These values indicate that T_1 is being dominated by the rotational correlation time (τ_r) or electron relaxation time (τ_s) or a combination of both. Bertini and co-workers[40,41,66] have extensively studied the dimeric metal complexes that have superexchange interactions with $|2J| > kT$ and $|2J| \approx kT$. According to them, longitudinal (T_{1M}) and transverse relaxation (T_{2M}) times of copper(II) homodimers are controlled by the population distribution in the $S = 0$ and $S = 1$ states rather than by a significant decrease in an electron relaxation time (τ_s). The relatively narrow lines observed in our systems may be due to appreciable population of the diamagnetic ground state. In our systems, by using eq 16, τ_r values of 2.22×10^{-10} s and 1.92×10^{-10} s are obtained for **1** and **2**. From our τ_c data and the error on the estimate of τ_r, τ_s can be anywhere between the monomeric value and $\sim 5 \times 10^{-10}$ s. Hence, no conclusions about the shortening of τ_s in these systems can be made from the data.

Conclusions

In this article we have observed hyperfine shifted ^{1}H NMR signals for three strongly antiferromagnetically coupled binuclear copper(II) complexes. By using the chemical shifts the exchange coupling constant ($-2J$) in solution has been calculated, which is compared with the solid state susceptibility measured by SQUID measurement. The structures and magnetic properties of all three reported complexes support a general correlation with the antiferromagnetic coupling constants as evidenced by both solid and solution studies. The exchangeable N−H and μ-hydroxy protons provide important chemical shifts and T_1 information for similar protons residing in metalloprotein active sites. The relaxation process for the dicopper system is mostly dominated by a dipolar mechanism. This allows T_1 values to be used as a measure of the distance for any given proton residing in the dicopper(II) center complexes. These data taken collectively suggest that ^{1}H NMR spectroscopy is an excellent structural and magnetic probe of dicopper(II) complexes in solution.

Acknowledgment. We thank the Department of Science and Technology, Government of India, New Delhi (SP/S1/F-47-90) for a grant to P.T.M. and CSIR for another grant to P.T.M. and financial assistance to A.A. in the form of a fellowship. We also thank Prof. Katsuae Inoue for magnetic susceptibility measurement and Dr. Babu Varghese and Dr. K. R. Justin Thomos for their help with X-ray crystallographic studies.

Supporting Information Available: Tables listing detailed crystallographic data, hydrogen atom positional parameters, anisotropic thermal parameters, and bond lengths and angles for **2** and a plot of chemical shifts vs T^{-1} for **1**, **2**, and **3**. X-ray crystallographic file, in CIF format, for **2**. This material is available free of charge via the Internet at http://pubs.acs.org.

IC9803356

(64) Banci, L.; Bertini, I.; Luchinat, C. *Nuclear and Electronic Relaxation. The magnetic nuclear-unpaired electron coupling in solution*; VCH: Weinheim, 1991.
(65) Bertini, I.; Luchinat, C.; Brown, R. D., III; Koenig, S. H. *J. Am. Chem. Soc.* **1989**, *111*, 3532.
(66) Bertini, I.; Banci, L.; Brown, R. D., III; Koenig, S. H.; Luchinat, C. *Inorg. Chem.* **1988**, *27*, 951.